

Effects of Strontium, Barium and Tin Doping on Electrical Properties of Calcium Titanate Ceramics for Capacitor Applications

May Kalayar Kyaing¹, Amy Aung², Ohnmar Swe³, Shwe Sin Oo⁴

Abstract

Strontium doped calcium titanate ($\text{Ca}_{0.9}\text{Sr}_{0.1}\text{TiO}_3$), barium doped calcium titanate ($\text{Ca}_{0.9}\text{Ba}_{0.1}\text{TiO}_3$) and tin doped calcium titanate ($\text{CaSn}_{0.1}\text{Ti}_{0.9}\text{O}_3$) ceramics were synthesized using a conventional solid-state reaction method. The aim of this paper is to investigate the effects of Sr, Ba and Sn on the crystal structures, surface morphologies and dielectric properties of CaTiO_3 ceramics. The crystallographic phases of the ceramics were identified by X-ray diffractometer (XRD) and confirmed that all the ceramics were crystallized into orthorhombic perovskite phase. The surface morphologies and average grain sizes of the ceramics were determined using scanning electron microscopy (SEM) and verified that the crystallite particles were agglomerated form. The average grain sizes were found to be ranging from 0.383 μm to 0.436 μm . The capacitance-voltage (C-V) measurements were performed at the frequency range from 1 kHz to 1000 kHz using a LCR meter. The highest dielectric constant was occurred in the $\text{CaSn}_{0.1}\text{Ti}_{0.9}\text{O}_3$ ceramic at the frequency range of 1 kHz. The dielectric constant is an important parameter of a dielectric material for the technological application of energy and data storage. From $1/C^2$ versus V graph, the effective dopant concentrations of the ceramics were also evaluated. The effective dopant concentrations of the ceramics were changed with the different doping materials and the maximum value was observed in the $\text{CaSn}_{0.1}\text{Ti}_{0.9}\text{O}_3$ ceramic.

Keywords: *Doped CaTiO_3 ceramics, LCR meter, dielectric constant, effective dopant concentration*

Introduction

Titanates as members of the perovskite structure family are well known ferroelectric materials with superior dielectric properties. Among all the titanates, calcium titanate (CaTiO_3) has become a strong candidate for the interest of scientific community due to its interesting dielectric properties and recently observed luminescence properties. Similar to other ceramics, properties of this material largely depend on the method of preparation, thermal treatments and doping with other additive oxides. Distortion of the material structure often occurs as a result of the introduction of dopants into the crystal lattice sites. This is also accompanied by an increase of charged ions [1]. Capacitor is an essential component to realize charge storage and decoupling for increasing transmission speed of integrated circuit. However, the limitation of capacitor area requires high capacitance density for embedded capacitors, thus promoting the blossom of dielectric materials with giant dielectric constant [2].

Ceramic materials with high dielectric permittivity and low dielectric losses have attracted attention because of their important applications in the electrical and electronic industries. In particular, perovskite based ceramic materials such as barium titanate and lead zirconium titanate etc., are widely used in capacitors due to their excellent dielectric properties [3]. For next-generation capacitive electrical energy storage applications, materials with high dielectric permittivity, low dielectric loss, and high dielectric breakdown strength are essential for high gravimetric energy storage capacity. High-energy density storage capacitors, by definition, store more energy per unit volume than common capacitors. These capacitors play a key role in stationary power systems, mobile electronic devices, hybrid electric vehicles, and pulsed power applications due to their reliability and fast charge-discharge characteristics [4]. The advanced technology requires a material with giant dielectric value to reduce the size

¹ Dr., Lecturer, Department of Physics, University of Yangon

² Dr., Lecturer, Department of Physics, University of Yangon

³ Dr., Associate Professor, Department of Physics, University of Yangon

⁴ Dr., Associate Professor, Department of Environment and Water Studies, University of Yangon

of electronic components, whereas the effective performance of these electronic components requires substantially low dielectric loss. High dielectric constant materials have numerous important applications in electronic devices such as capacitors, static and dynamic random access memories [5].

CaTiO_3 powder is usually mixed with various types of materials in order to obtain the better performances and a good control over a grain size and electrical characteristics of ceramics. Doping is an effective way to improve the electrical performance of electroceramics [6]. The aim of this paper is to investigate the doping effects of strontium (Sr), barium (Ba) and tin (Sn) on the structural and electrical properties of calcium titanate (CaTiO_3) ceramics.

Materials and Methods

$\text{Ca}_{0.9}\text{Sr}_{0.1}\text{TiO}_3$, $\text{Ca}_{0.9}\text{Ba}_{0.1}\text{TiO}_3$ and $\text{CaSn}_{0.1}\text{Ti}_{0.9}\text{O}_3$ powders were prepared by conventional solid state reaction of calcium oxide CaO, titanium oxide TiO_2 , strontium oxide SrO, barium oxide BaO and tin oxide SnO_2 materials. The compounds were mixed in an agate mortar with addition of acetone to obtain a homogeneous mixture. The powders were pressed into pellets of diameter 1.3 cm and the pellets were heated at at 900 °C for 3 hours. X-ray diffraction (XRD) was conducted at room temperature to determine the crystal structure of all the ceramics and the investigation of the surface morphologies of the ceramics was done by scanning electron microscope (SEM). The electrical properties of ceramics such as dielectric constant and dielectric loss were studied by using a LCR meter as presented in Figure 1. The ceramics were measured in the frequency range from 1 kHz to 1000 kHz at room temperature. From $1/C^2$ versus V graph, the effective dopant concentrations (N_D) of the ceramics were also examined.



Figure 1 Capacitance-voltage measurement of the ceramics using LCR meter

Results and Discussion

Structural analysis

Figure 2 (a), (b) and (c) show the XRD patterns obtained from $\text{Ca}_{0.9}\text{Sr}_{0.1}\text{TiO}_3$, $\text{Ca}_{0.9}\text{Ba}_{0.1}\text{TiO}_3$ and $\text{CaSn}_{0.1}\text{Ti}_{0.9}\text{O}_3$ ceramics with the angle (2θ) in the range from 10° to 70° . The major intense peak was observed at (1 0 1) plane in the three samples and the most intense peak was occurred at (1 0 1) plane of the $\text{CaSn}_x\text{Ti}_{1-x}\text{O}_3$ ceramics. XRD profiles confirmed the presence of Sr, Ba and Sn doped CaTiO_3 materials in the ceramics and also indicated that all the ceramics were crystallized into orthorhombic perovskite phase. The average crystallite size was calculated by using Debye Scherrer method [7]. A small value of FWHM implies a high crystallinity of the sample. The calculated average crystallite sizes were 31.63, 39.92 and 38.17 nm, corresponding to the $\text{Ca}_{0.9}\text{Sr}_{0.1}\text{TiO}_3$, $\text{Ca}_{0.9}\text{Ba}_{0.1}\text{TiO}_3$ and $\text{CaSn}_{0.1}\text{Ti}_{0.9}\text{O}_3$ ceramics, respectively. The lattice parameter and crystallite size of the ceramics were changed with the different doping materials. The variation of the lattice parameter indicated that the doped ion substitutes in the A site or B site of ABO_3 perovskite structure. Thus, XRD analyses were employed in order to estimate the influence of the doping materials on the lattice parameters of the ceramics. The structural properties of the ceramics are presented in Table 1.

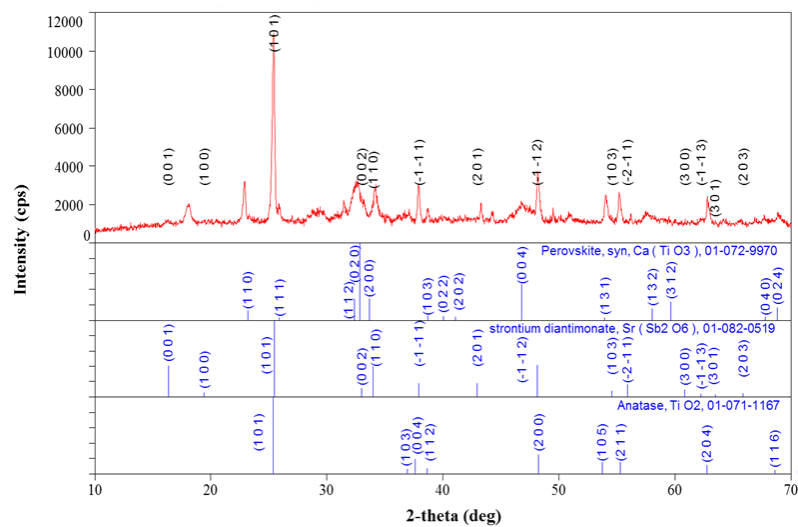


Figure 2(a) XRD pattern of $\text{Ca}_{0.9}\text{Sr}_{0.1}\text{TiO}_3$ ceramic

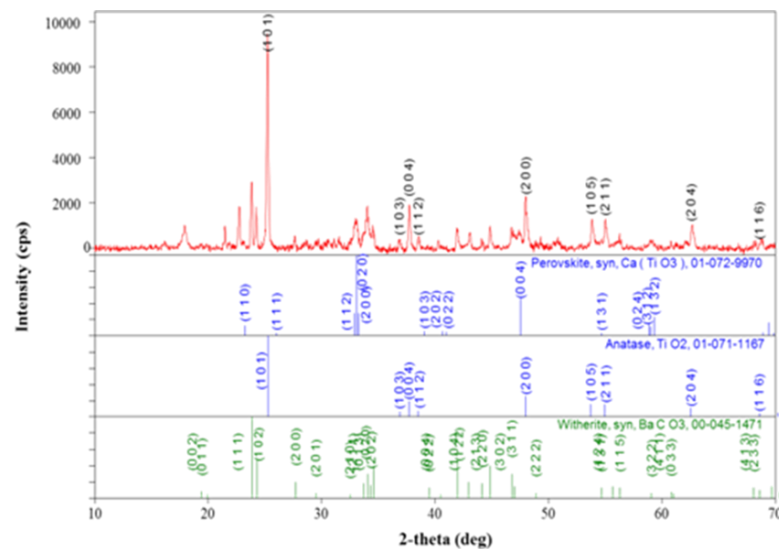


Figure 2(b) XRD pattern of $\text{Ca}_{0.9}\text{Ba}_{0.1}\text{TiO}_3$ ceramic

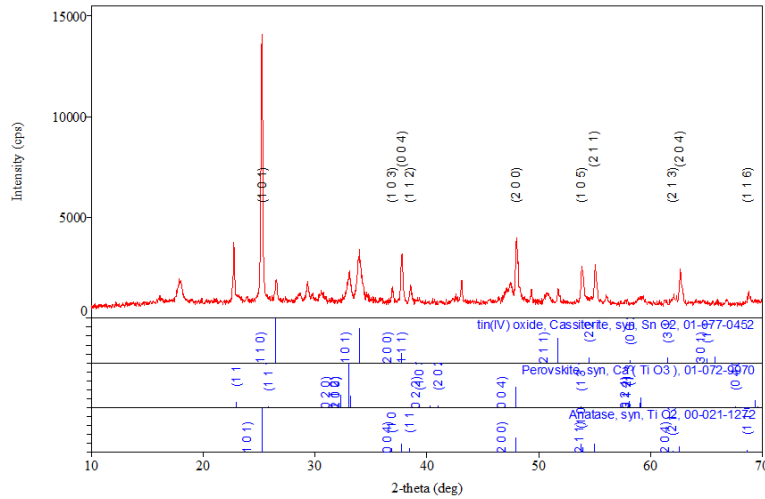
Figure 2(c) XRD pattern of $\text{CaSn}_{0.1}\text{Ti}_{0.9}\text{O}_3$ ceramic

Table 1 Structural properties of the ceramics

Ceramic	Crystal structure	Lattice parameter			Average crystallite size D (nm)
		a (Å)	b (Å)	c (Å)	
$\text{Ca}_{0.9}\text{Sr}_{0.1}\text{TiO}_3$	Orthorhombic	5.4871	5.5053	7.7251	31.63
$\text{Ca}_{0.9}\text{Ba}_{0.1}\text{TiO}_3$	Orthorhombic	5.3805	5.4819	7.6918	39.92
$\text{CaSn}_{0.1}\text{Ti}_{0.9}\text{O}_3$	Orthorhombic	5.3997	5.4395	7.5794	38.17

Surface Morphological Analysis

SEM examined the surface morphological features of the ceramics. The SEM images of the $\text{Ca}_{0.9}\text{Sr}_{0.1}\text{TiO}_3$, $\text{Ca}_{0.9}\text{Ba}_{0.1}\text{TiO}_3$ and $\text{CaSn}_{0.1}\text{Ti}_{0.9}\text{O}_3$ ceramics annealed at 900°C are shown in Figure 3 (a-c). These ceramics exhibited an almost spherical morphology and have a porous agglomerated form. The particle size of the ceramics was in the range from $0.383\ \mu\text{m}$ to $0.436\ \mu\text{m}$ and was found to slightly changes with the different doping material of the ceramics. The grain size of $\text{Ca}_{0.9}\text{Sr}_{0.1}\text{TiO}_3$ ceramic was smaller than that of the other ceramics. The average grain size of the ceramics are listed in Table 2.

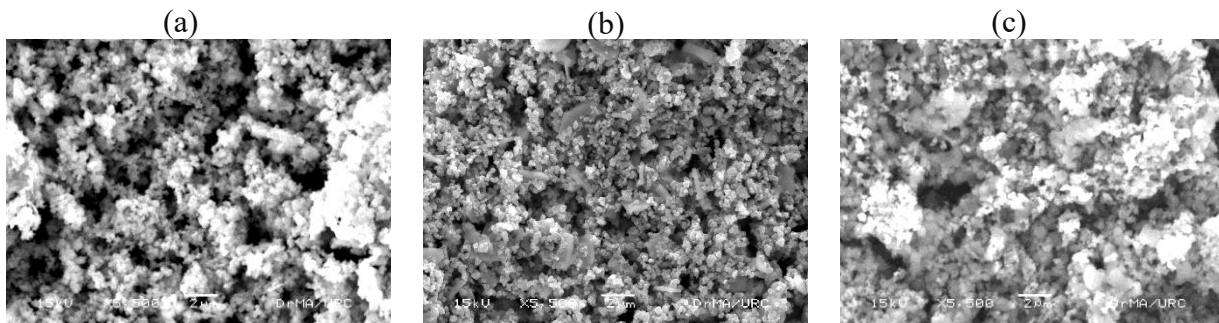
Figure 3 SEM images of (a) $\text{Ca}_{0.9}\text{Sr}_{0.1}\text{TiO}_3$ (b) $\text{Ca}_{0.9}\text{Ba}_{0.1}\text{TiO}_3$ and (c) $\text{CaSn}_{0.1}\text{Ti}_{0.9}\text{O}_3$ ceramics

Table 2 Average grain size of the $\text{Ca}_{0.9}\text{Sr}_{0.1}\text{TiO}_3$, $\text{Ca}_{0.9}\text{Ba}_{0.1}\text{TiO}_3$ and $\text{CaSn}_{0.1}\text{Ti}_{0.9}\text{O}_3$ ceramics

Ceramic	Grain Size (μm)
$\text{Ca}_{0.9}\text{Sr}_{0.1}\text{TiO}_3$	0.383
$\text{Ca}_{0.9}\text{Ba}_{0.1}\text{TiO}_3$	0.436
$\text{CaSn}_{0.1}\text{Ti}_{0.9}\text{O}_3$	0.427

Dielectric Properties

The frequency responses for dielectric properties of the $\text{Ca}_{0.9}\text{Sr}_{0.1}\text{TiO}_3$, $\text{Ca}_{0.9}\text{Ba}_{0.1}\text{TiO}_3$ and $\text{CaSn}_{0.1}\text{Ti}_{0.9}\text{O}_3$ ceramics were measured in detail through an impedance analyzer with the frequency range from 1 kHz to 1000 kHz. The ability of a dielectric material to store energy under the influence of an electric field results from the separation and alignment of electric charges brought about by that field. The larger the dipole moment, the separation of charges in the direction of the field, and the larger the number of these dipoles, the higher the material's dielectric constant. The values of dielectric constant (κ) were calculated by the equations below,

$$C_0 = \varepsilon_0 \frac{A}{t} \quad (1)$$

$$\kappa = C/C_0 \quad (2)$$

where, C = capacitance using the material as the dielectric in the capacitor,

C_0 = capacitance using vacuum as the dielectric,

ε_0 = permittivity of free space ($8.85 \times 10^{-12} \text{ F/m}$) [8].

At low frequencies, the dielectric constants of the ceramics were high and decreased gradually to a high frequency. It was found that all the ceramic samples have good dielectric properties and the dielectric constant of the $\text{CaSn}_{0.1}\text{Ti}_{0.9}\text{O}_3$ ceramic was larger than that of the $\text{Ca}_{0.9}\text{Sr}_{0.1}\text{TiO}_3$ and $\text{Ca}_{0.9}\text{Ba}_{0.1}\text{TiO}_3$ ceramics at the same doping amount. Figure 4 shows the dielectric constant of $\text{Ca}_{0.9}\text{Sr}_{0.1}\text{TiO}_3$, $\text{Ca}_{0.9}\text{Ba}_{0.1}\text{TiO}_3$ and $\text{CaSn}_{0.1}\text{Ti}_{0.9}\text{O}_3$ ceramics as a function of frequency.

The energy loss in a dielectric is due to an alternating electric field, which is a material property rather than geometric property of a capacitor. Usually the dielectric loss expressed as the dissipation factor or loss tangent. Figure 5 shows the dielectric loss of $\text{Ca}_{0.9}\text{Sr}_{0.1}\text{TiO}_3$, $\text{Ca}_{0.9}\text{Ba}_{0.1}\text{TiO}_3$ and $\text{CaSn}_{0.1}\text{Ti}_{0.9}\text{O}_3$ ceramics as a function of frequency. The values of the dielectric constant and dielectric loss of the ceramics are summarized in Table 3.

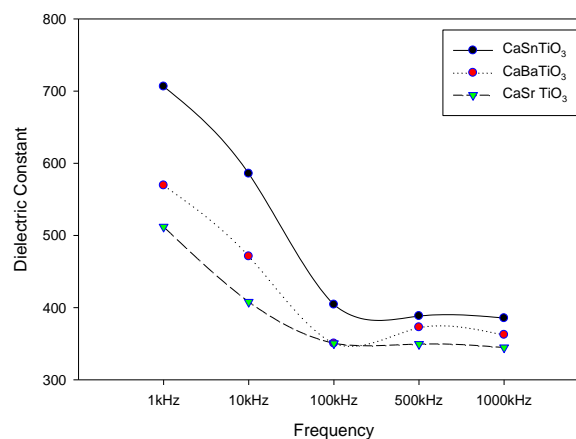


Figure 4 The dielectric constant of the $\text{Ca}_{0.9}\text{Sr}_{0.1}\text{TiO}_3$, $\text{Ca}_{0.9}\text{Ba}_{0.1}\text{TiO}_3$ and $\text{CaSn}_{0.1}\text{Ti}_{0.9}\text{O}_3$ ceramics as a function of frequency

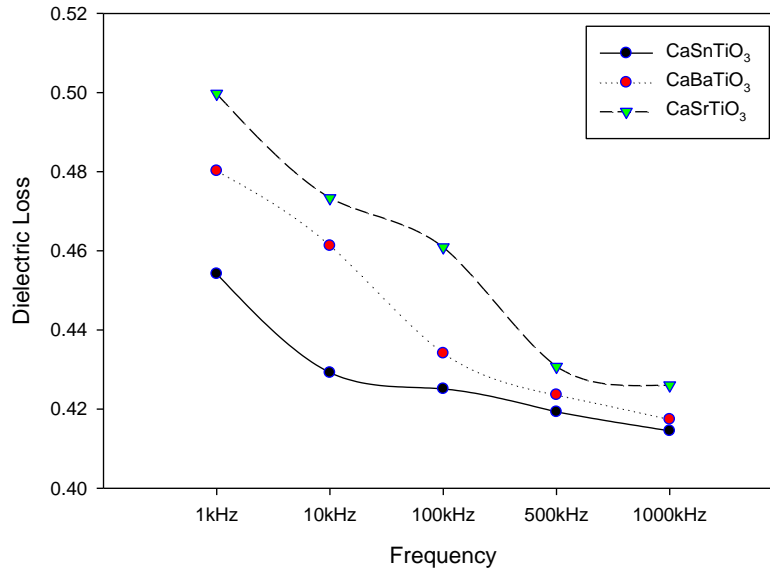


Figure 5 The dielectric loss of the $\text{Ca}_{0.9}\text{Sr}_{0.1}\text{TiO}_3$, $\text{Ca}_{0.9}\text{Ba}_{0.1}\text{TiO}_3$ and $\text{CaSn}_{0.1}\text{Ti}_{0.9}\text{O}_3$ ceramics as a function of frequency

Table 3 The dielectric constants and dielectric loss of the ceramics

Ceramic	Dielectric constant	Dielectric loss (%)
$\text{Ca}_{0.9}\text{Sr}_{0.1}\text{TiO}_3$	512.144	0.4997
$\text{Ca}_{0.9}\text{Ba}_{0.1}\text{TiO}_3$	569.176	0.4802
$\text{CaSn}_{0.1}\text{Ti}_{0.9}\text{O}_3$	706.135	0.4542

Capacitance-Voltage Analysis

The electrical properties of the $\text{Ca}_{0.9}\text{Sr}_{0.1}\text{TiO}_3$, $\text{Ca}_{0.9}\text{Ba}_{0.1}\text{TiO}_3$ and $\text{CaSn}_{0.1}\text{Ti}_{0.9}\text{O}_3$ ceramics were investigated from capacitance-voltage measurements by using a LCR meter. The built in voltage (V_{bi}) of the ceramics was examined from $1/C^2$ versus V graph. The effective dopant concentration (N_D) near the junction was determined from the equation (3),

$$\frac{1}{C^2} = \frac{2(V_{bi} - V)}{A^2 q \epsilon_s N_D} \quad (3)$$

The depletion region is formed from a conducting region by removal of all free charge carriers, leaving none to carry a current. The depletion region is a key to explaining modern semiconductor electronics such as diodes, bipolar junction transistors, field effect transistors and variable capacitance diodes, all rely on depletion region phenomena. The only elements left in the depletion region are ionized donor or acceptor impurities. The depletion layer width of the space charge region (W) was calculated by the equation (4),

$$W = \frac{\epsilon_s A}{C} \quad (4)$$

where “ A ” is the area of the ceramic and “ ϵ_s ” is the permittivity of the material [9]. Figure 6(a), (b) and (c) show the $1/C^2$ versus V graphs of the $\text{Ca}_{0.9}\text{Sr}_{0.1}\text{TiO}_3$, $\text{Ca}_{0.9}\text{Ba}_{0.1}\text{TiO}_3$ and $\text{CaSn}_{0.1}\text{Ti}_{0.9}\text{O}_3$ ceramics. The values of the built in voltage, effective dopant concentration and depletion layer width of the ceramics are listed in Table 4.

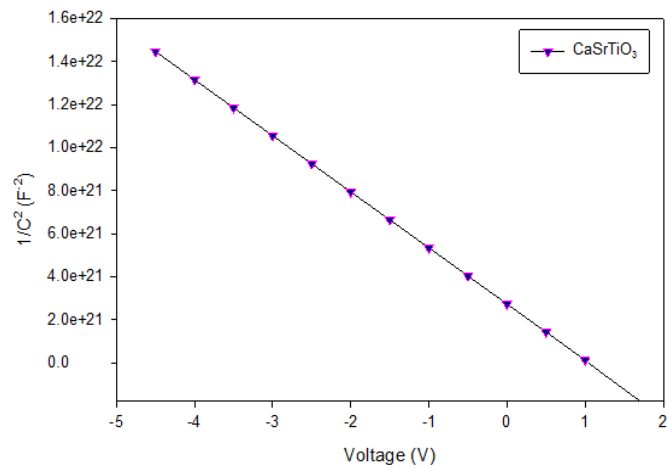
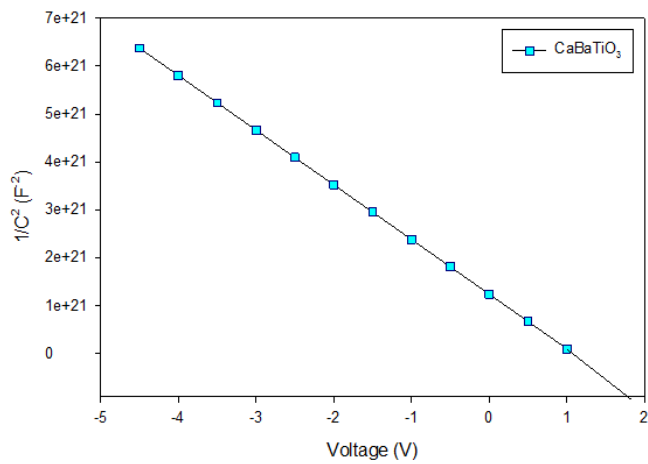
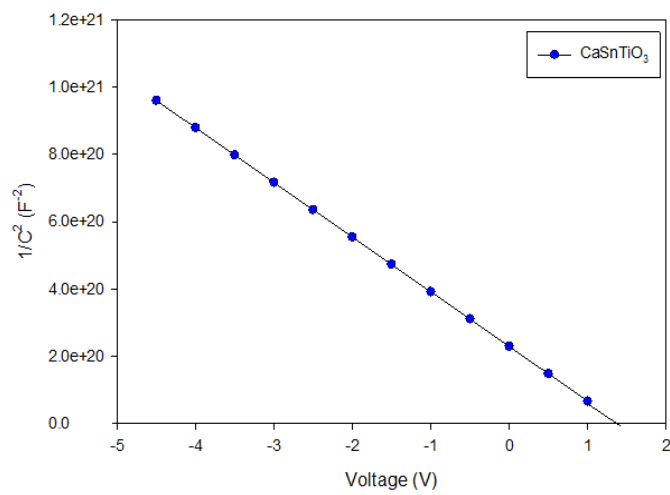
Figure 6(a) Plot of $1/C^2$ versus V for $\text{Ca}_{0.9}\text{Sr}_{0.1}\text{TiO}_3$ ceramicFigure 6(b) Plot of $1/C^2$ versus V for $\text{Ca}_{0.9}\text{Ba}_{0.1}\text{TiO}_3$ ceramicFigure 6(c) Plot of $1/C^2$ versus V for $\text{CaSn}_{0.1}\text{Ti}_{0.9}\text{O}_3$ ceramic

Table 4 Built in voltage (V_{bi}), effective dopant concentration (N_D) and depletion layer width (W) of the the ceramics

Ceramic	V_{bi} (V)	N_D (cm^{-3})	W (cm)
$\text{Ca}_{0.9}\text{Sr}_{0.1}\text{TiO}_3$	1.626	1.18×10^{13}	0.0450
$\text{Ca}_{0.9}\text{Ba}_{0.1}\text{TiO}_3$	1.765	2.42×10^{14}	0.0453
$\text{CaSn}_{0.1}\text{Ti}_{0.9}\text{O}_3$	1.329	5.98×10^{14}	0.0416

Conclusion

The perovskite ceramics of $\text{Ca}_{0.9}\text{Sr}_{0.1}\text{TiO}_3$, $\text{Ca}_{0.9}\text{Ba}_{0.1}\text{TiO}_3$ and $\text{CaSn}_{0.1}\text{Ti}_{0.9}\text{O}_3$ samples were successfully synthesized by conventional solid-state reaction method. XRD profiles confirmed the presence of Sr, Ba and Sn doped CaTiO_3 materials in the ceramics and also indicated that all the ceramics were crystallized into orthorhombic perovskite phase. SEM images showed that these ceramics exhibited an almost spherical morphology and have a porous agglomerated form. The lattice parameters and grain sizes of the ceramics were changed with the different doping materials. From the capacitance-voltage measurements, the values of dielectric constant of the $\text{Ca}_{0.9}\text{Sr}_{0.1}\text{TiO}_3$, $\text{Ca}_{0.9}\text{Ba}_{0.1}\text{TiO}_3$ and $\text{CaSn}_{0.1}\text{Ti}_{0.9}\text{O}_3$ ceramics were observed as 512.14, 569.176 and 706.135, respectively. The results showed that all the ceramic samples have good dielectric properties. The effective dopant concentrations of the $\text{Ca}_{0.9}\text{Sr}_{0.1}\text{TiO}_3$, $\text{Ca}_{0.9}\text{Ba}_{0.1}\text{TiO}_3$ and $\text{CaSn}_{0.1}\text{Ti}_{0.9}\text{O}_3$ ceramics were found to be $1.18 \times 10^{13} \text{cm}^{-3}$, $2.42 \times 10^{14} \text{cm}^{-3}$ and $5.98 \times 10^{14} \text{cm}^{-3}$, respectively. The dielectric properties and the effective dopant concentrations of $\text{CaSn}_{0.1}\text{Ti}_{0.9}\text{O}_3$ ceramic were better than that of the $\text{Ca}_{0.9}\text{Sr}_{0.1}\text{TiO}_3$, $\text{Ca}_{0.9}\text{Ba}_{0.1}\text{TiO}_3$ ceramics. Based on the results, these samples have good electrical properties for the fabrication of capacitors used in microelectronic applications.

Acknowledgements

The authors would like to thank Dr Tin Maung Tun, Rector, University of Yangon, for his permission to this paper. We also wish to thank Dr Khin Chit Chit, Dr Cho Cho and Dr Thidar Aye, Pro-rectors, University of Yangon, for their kind permission to this paper.

We are very grateful to Professor Dr Yin Maung Maung, Head of Department of Physics, University of Yangon, for his kind encouragement. We would like to express our sincere thanks to Dr Ye Chan, Professor and Head, Universities' Research Center, Dr Min Maung Maung, Dr Cho Cho Thet and Dr Nyein Thida, Professors, Department of Physics, University of Yangon, for their valuable advice to this paper.

References

- M. Ahmadipour, M. F. Ain, and Z. A. Ahmad, "A Short Review on Copper Calcium Titanate (CCTO) Electroceramic: Synthesis, Dielectric Properties, Film Deposition, and Sensing Application," *Nano-Micro Lett.*, vol. 8, no. 4, pp. 291–311, 2016.
- N. D. Reynolds, C. D. Panda, and J. M. Essick, "Capacitance-voltage profiling : Research-grade approach versus low-cost alternatives," vol. 97202, no. July 2013, pp. 196–205, 2014.
- V. S. Puli, A. Kumar, D. B. Chrisey, M. Tomozawa, J. F. Scott, and R. S. Katiyar, "Barium zirconate-titanate/barium calcium-titanate ceramics via sol-gel process: Novel high-energy-density capacitors," *J. Phys. D. Appl. Phys.*, vol. 44, no. 39, 2011.
- R. Ulrich, L. Schaper, D. Nelms, and M. Leftwich, "Comparison of paraelectric and ferroelectric materials for applications as dielectrics in thin film integrated capacitors," *Int. J. microcircuits Electron. Packag.*, vol. 23, no. 2, pp. 172–181, 2000.
- O. a a Abdelal, A. a Hassan, and M. E. Ali, "Dielectric Properties of Calcium Copper Titanates ($\text{CaCu}_3\text{Ti}_4\text{O}_{12}$) Synthesized by Solid State Reaction," *Int. J. Adv. Res. Chem. Sci.*, vol. 45, no. 2, pp. 354–361, 2014.

- V. S. Puli *et al.*, “Core-shell like structured barium zirconium titanate-barium calcium titanate–poly(methyl methacrylate) nanocomposites for dielectric energy storage capacitors,” *Polymer (Guildf.)*, vol. 105, pp. 35–42, 2016.
- S. Wang *et al.*, “Graphene-coated copper calcium titanate to improve dielectric performance of PPO-based composite,” *Mater. Lett.*, vol. 233, pp. 355–358, 2018.
- S. Equipment, “User’s Manual Study of dielectric constant model: Scientific Equipment & Services, Dielectric and curie temperature measurement of ferroelectric ceramics,” *Magnesium*, 2000.
- J. P. Singh *et al.*, “Correlation between the dielectric properties and local electronic structure of copper doped calcium titanate,” *J. Alloys Compd.*, vol. 572, pp. 84–89, 2013.

